

**CYG X-3: NOT SEEN IN HIGH-ENERGY GAMMA RAYS BY COS-B**

W.Hermsen<sup>1</sup>, K.Bennett<sup>6</sup>, G.F.Bignami<sup>2</sup>, J.B.G.M.Bloemen<sup>1a</sup>, R.Buccheri<sup>3</sup>,  
P.A.Caraveo<sup>2</sup>, H.A.Mayer-Hasselwander<sup>4</sup>, M.E. Özel<sup>b</sup>, A.M.T.Pollock<sup>5c</sup>,  
A.W.Strong<sup>4</sup>

The Caravane Colaboration for the COS-B satellite:

<sup>1</sup> Laboratory for Space Research Leiden, Leiden, The Netherlands

<sup>2</sup> Istituto di Fisica Cosmica del CNR, Milano, Italy

<sup>3</sup> Istituto di Fisica Cosmica e Informatica del CNR, Palermo, Italy

<sup>4</sup> Max Planck Institut für Physik und Astrophysik, Institut für  
Extraterrestrische Physik, Garching-bei-München, Germany

<sup>5</sup> Service d'Astrophysique, Centre d'Etudes Nucléaires de Saclay, France

<sup>6</sup> Space Science Department of the European Space Agency, ESTEC,  
Noordwijk, The Netherlands

<sup>a</sup> Sterrewacht Leiden, Huygens Laboratorium, Leiden, The Netherlands

<sup>b</sup> Max-Planck-Institut für Radioastronomie, Bonn, Germany.

<sup>c</sup> Department of Space Research, University of Birmingham, Birmingham,  
England

**1. Introduction.** Cyg X-3 is a very peculiar source, studied over the entire electromagnetic spectrum. Considering here the high-energy end of its spectrum the source has been found to be modulated with its characteristic 4.8 h period in the hard X-ray band up to  $\sim 200$  keV (e.g. 13), and in the very-high-energy gamma-ray range ( $\sim 10^{11}$  to  $10^{14}$  eV; e.g. review 6), and the ultra-high-energies (above  $10^{14}$  eV; e.g. 8,14). However, the experimental status regarding the detection of high-energy ( $\sim 5 \times 10^7$ – $5 \times 10^9$  eV) gamma rays from Cyg X-3, modulated with its characteristic 4.8 h period, is confusing. The first claim of a detection of periodic emission at high-energy gamma rays from Cyg X-3 was based on only 15 excess counts ( $E > 40$  MeV) over an expected background of 47 counts collected during two balloon flights<sup>3</sup>. This result was confirmed by the SAS-2 team<sup>5</sup> for energies above 35 MeV. However, analysis of successive COS-B observations of the Cyg-X region ( $E > 50$  MeV) did not reveal the source<sup>1,4,15</sup>, while the X-ray detector aboard COS-B detected Cyg X-3 to be in a high state of activity during some of the observation periods<sup>17</sup>. In this paper we summarize the results obtained from a more sensitive analysis of the complete COS-B data on Cyg X-3.

**2. Analysis and Results.** COS-B had Cyg X-3 within its field of view during 7 observation periods between 1975 and 1982 for in total  $\sim 300$  days. In the skymaps ( $70 \text{ MeV} < E < 5000 \text{ MeV}$ ) of the Cyg-X region produced for each of these observations and in the summed map, a broad complex structure is visible in the region  $72^\circ \lesssim l \lesssim 85^\circ$ ,  $|b| \lesssim 5^\circ$  (see e.g. Mayer-Hasselwander et al.<sup>9</sup>). No resolved source structure is visible at the position of Cyg X-3, but a weak signal from Cyg X-3 could be hidden in the structured gamma-ray background. Therefore, the data has been searched for a 4.8 h timing signature, as well as for a source signal in the sky map in addition to the diffuse background structure as estimated from tracers of atomic and molecular gas.

a) Timing analysis. The arrival times of gamma-ray photons ( $70 \text{ MeV} < E < 5000 \text{ MeV}$ ) originating from a small region around the position of Cyg X-3

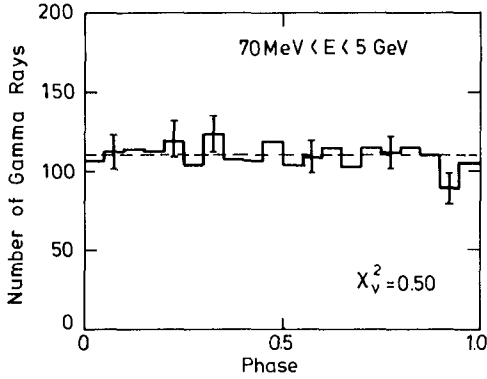


Figure 1: Phase histogram of the arrival time, folded modulo  $\sim 4.8$  h period, of gamma rays with energy  $70 \text{ MeV} < E < 5000 \text{ MeV}$  originating from a small region centered on Cyg X-3. Data from 7 COS-B observations are used. The average level is indicated.

have been folded using an ephemeris derived from the COS-B X-ray data by Van der Klis and Bonnet-Bidaud<sup>17</sup>. The gamma-ray photons are selected using the background-sensitive selection algorithm proposed by Özel and Mayer-Hasselwander<sup>11</sup>. This algorithm optimizes the signal-to-noise ratio taking into account the COS-B instrumental point-spread function and the structure measured in the surrounding sky region, both as a function of energy. In order to verify that the background levels in the phase histograms (20 bins) are flat for each observation, also background samples have been folded with the 4.8 h period. For each observation period the phase histograms for the background samples and the 'source' samples were statistically consistent with flat distributions (see Table 1). Therefore, only upper limits on the modulated emission could be determined. For these flat distributions these upper limits are primarily a function of the expected duty cycle. We have calculated upper limits for three cases: the phase interval 0.05-0.85 (I) over which the X-ray emission has been detected, and the phase intervals 0.20-0.30 (II) and 0.50-0.70 (III), in which detections of a signal from Cyg X-3 has been reported at very-high-energy and ultra-high-energy gamma rays. Table 1 gives the  $2\sigma$  upper limits for the single observations and for the combined data. Figure 1 shows the corresponding combined light curve. The upper limits are for the X-ray phases (I) one order of magnitude below a power-law interpolation between the very-high-energy data points and the X-ray results, and for the ultra-high-energy phases two orders of magnitude below this interpolation (e.g. 14).

Table 1: Reduced  $\chi^2$  values for 20-bin phase histograms for background (bg) and 'source' (s) samples and  $2\sigma$  upper limits ( $\text{ph cm}^{-2} \text{ s}^{-1}$ ) to the modulated (4.8 h) flux (70-5000 MeV) from Cyg X-3 for the three phase intervals given in the text.

Obs. number	Epoch of measurement	$\chi^2_{\text{bg}}$	$\chi^2_{\text{s}}$	I ( $10^{-6}$ )	II ( $10^{-7}$ )	III ( $10^{-7}$ )
4	75/11/28-75/12/24	0.69	0.80	1.8	3.0	2.8
22	77/06/08-77/07/15	1.05	1.87	2.2	4.3	4.6
36	78/11/03-78/12/11	0.76	0.31	1.6	3.9	3.8
51	80/05/14-80/06/24	1.21	0.73	2.7	4.6	2.4
55	80/10/17-80/11/04	1.11	0.75	3.1	0.9	5.0
60	81/06/03-81/07/24	0.79	1.22	2.7	1.9	2.2
63	81/11/03-82/02/18	0.64	0.50	1.0	2.5	0.4
<b>Total</b>				1.0	1.0	1.1

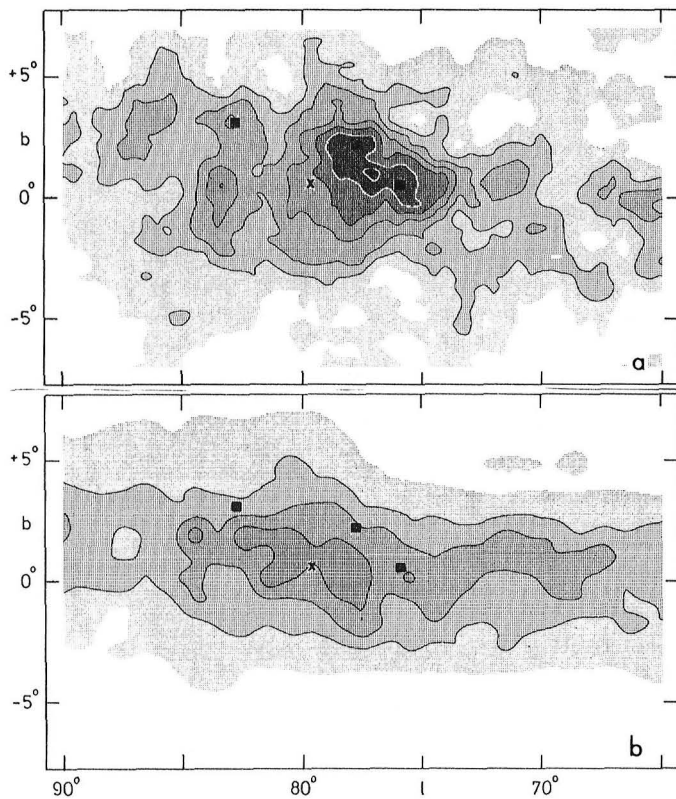


Figure 2: Gamma-ray intensity ( $E > 500$  MeV) distributions in the Cyg-X region. Contour levels: 4, 6, ..., 12, 14  $\times 10^{-5}$  photon  $\text{cm}^{-2}$   $\text{s}^{-1}$   $\text{sr}^{-1}$ , first step in grey scale at  $2 \times 10^{-5}$  photon  $\text{cm}^{-2}$   $\text{s}^{-1}$   $\text{sr}^{-1}$ . a) Measured by COS-B. b) Estimated from the total gas distribution using HI and CO data. ■: Position of gamma-ray sources<sup>12</sup> not explained by the gas. x: Cyg X-3 position.

b) Spatial Analysis. The COS-B team has shown that the structured emission in the Cyg-X region can be explained as being the sum of (i) diffuse emission from the interaction between relativistic cosmic rays and the total-gas distribution and (ii) two pointlike sources which cannot be explained by the gas distribution<sup>12</sup> (see Figures 2 and 3c). Figure 2a shows a contour plot of the gamma-ray intensities in the Cyg-X region for energies above 500 MeV (the highest COS-B energies with the best angular resolution).

A combination of HI measurements with the recent Columbia large-scale CO survey (ref's in 2, 12) allows a detailed estimate of the diffuse emission above which any sources appear (see Figure 2b). Using Bloemen et al's<sup>2</sup> model of the diffuse emission we have used a likelihood method<sup>12</sup> to test the presence of a point source at the position of Cyg

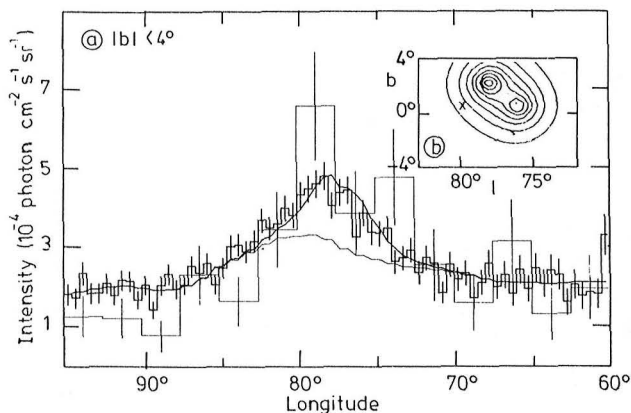


Figure 3: a) Normalized COS-B (thick) and SAS-2 (thin) histograms ( $E > 100$  MeV; isotropic background levels are subtracted, for SAS-2 from 7, 16). Thick curve: sum of the expected diffuse gamma-ray emission and that from two sources<sup>12</sup>. Thin curve: diffuse emission only. b) Contourplot of source intensities contributing to Fig. 3a. x: Cyg X-3 position.

X-3, in addition to the total structure due to the diffuse emission and the two sources. The analysis was performed for the total COS-B data set in three energy ranges, treating the intensity of each component as free parameters. No evidence for the detection of Cyg X-3 was found; Table 2 gives  $2\sigma$  upper limits to the total flux.

**3. Discussion.** The COS-B upper limits are significantly lower than the flux of  $(4.4 \pm 1.1) \times 10^{-6}$  photon  $\text{cm}^{-2} \text{s}^{-1}$  for energies above 100 MeV reported from SAS-2 (Lamb et al.<sup>5</sup>). Lamb et al. identified in their analysis the total excess in the Cyg-X region with Cyg X-3, and, in addition, they claimed the total gamma-ray flux to be modulated with the 4.8 h period. However, the CO data (see Figure 2b) indicate that a significant fraction of the gamma rays are due to diffuse emission. Comparing the SAS-2 distribution with that measured by COS-B, we find no evidence for an excess in the SAS-2 case due to variable, modulated emission from Cyg X-3. Since there appears to be a systematic difference between the COS-B and SAS-2 absolute intensities in this region, the SAS-2 intensities being systematically lower as was already noticed by Mayer-Hasselwander<sup>10</sup>, we normalized the total SAS-2 intensity measured in the longitude interval  $60^\circ < l < 95^\circ$  to that of COS-B. This comparison is shown in Figure 3. The shapes of the two distributions are evidently consistent, and the absolute levels agree everywhere within the  $\sim 1\sigma$  level. The conclusion which may be drawn from this comparison is, that in the total gamma-ray excess in the Cyg-X region, measured by COS-B and SAS-2, no contribution can be identified from Cyg X-3 at the flux level reported from SAS-2.

*Table 2:  $2\sigma$  upper limits to the total time-averaged gamma-ray flux from Cyg X-3 using the complete COS-B data.*

Energy range	$2\sigma$ upper limit
70-150 MeV	$7.5 \times 10^{-7}$ photon $\text{cm}^{-2} \text{s}^{-1}$
150-300 MeV	$6.5 \times 10^{-7}$ photon $\text{cm}^{-2} \text{s}^{-1}$
300-5000 MeV	$4.5 \times 10^{-7}$ photon $\text{cm}^{-2} \text{s}^{-1}$

#### References

1. Bennett et al. (1977), Astron. Astrophys. **59**, 273
2. Bloemen et al. (1985), Astron. Astrophys. subm., and OG3.1-6.
3. Galper et al. (1976) Sov. Astron. Letters **2**, No. 6, 206-208
4. Hermsen, W. (1983), Space Science Reviews **36**, 61-92
5. Lamb et al. (1977), Astron. J. Letters **212**, L63-66
6. Lamb, R.C. (1984), Proc. Workshop on Cosmic Ray Experiments for the Space Station Era, Baton Rouge, October 1984
7. Lebrun, F. Paul, J.A.: 1983, Astrophys. J. **266**, 276
8. Lloyd-Evans et al. (1983), Nature **305**, 784-787
9. Mayer-Hasselwander et al. (1982), Astron. Astrophys. **105**, 164-175
10. Mayer-Hasselwander, H.A. (1983), Space Science Reviews **36** 223-247
11. Özel, M.E. and Mayer-Hasselwander, H.A. (1983), Astron. Astrophys. **125**, 130-135.
12. Pollock et al. (1985), Astron. Astrophys. in press, and OG3.1-9
13. Reppin et al. (1979), Astrophys. J. **234**, 329
14. Samorski, M., and Stamm, W.: 1983, Astrophys. J. **268**, L17-L21
15. Swanenburg et al. (1981), Astrophys. J. Letters **243**, L69-L73
16. Thompson, D.J., Fichtel, C.E.: 1982, Astron. Astrophys. **109**, 352
17. Van der Klis, M., and Bonnet-Bidaud, J.M.: 1981, Astron. Astrophys. **95**, L5-L7